sustainability

MDPI

Article

Eco-Friendly Cellulose Nanofiber Extraction from Sugarcane Bagasse and Film Fabrication

Naresh Shahi [1], Byungjin Min [2,*], Bedanga Sapkota [3] and Vijaya K. Rangari [3,*]

[1] Integrative Biosciences Ph.D. Program, Tuskegee University, Tuskegee, AL 36088, USA; nshahi1164@tuskegee.edu
[2] Department of Food and Nutritional Sciences, Tuskegee University, Tuskegee, AL 36088, USA
[3] Department of Materials Science and Engineering, Tuskegee University, Tuskegee, AL 36088, USA; bsapkota@tuskegee.edu
* Correspondence: bmin@tuskegee.edu (B.M.); vrangari@tuskegee.edu (V.K.R.); Tel.: +1-334-727-8393 (B.M.); +1-334-724-4875 (V.K.R.)

Received: 6 July 2020; Accepted: 24 July 2020; Published: 27 July 2020

Abstract: The development of cost-effective cellulose fibers by utilizing agricultural residues have been attracted by the scientific community in the past few years; however, a facile production route along with minimal processing steps and a significant reduction in harsh chemical use is still lacking. Here, we report a straightforward ultrasound-assisted method to extract cellulose nanofiber (CNF) from fibrous waste sugarcane bagasse. X-ray diffraction-based crystallinity calculation showed 25% increase in the crystallinity of the extracted CNF (61.1%) as compared to raw sugarcane bagasse (35.1%), which is coherent with Raman studies. Field emission scanning electron microscopy (FE-SEM) images revealed thread-like CNF structures. Furthermore, we prepared thin films of the CNF using hot press and solution casting method and compared their mechanical properties. Our experiments demonstrated that hot press is a more effective way to produce high strength CNF films; Young's modulus of the thin films prepared from the hot press was ten times higher than the solution casting method. Our results suggest that a combination of ultrasound-based extraction and hot press-based film preparation is an efficient route of producing high strength CNF films.

Keywords: ultrasonication; CNF films; biomass; sustainable

1. Introduction

Plant-based biomass consists of lignocellulosic materials such as lignin, hemicellulose, and cellulose. Among plant-based biomass, agricultural by-products could serve as sustainable, renewable, and inexpensive raw materials to produce industrial biopolymers [1]. For instance, sugarcane bagasse (SCB), a residue produced from the sugarcane industry, contains approximately 40 to 50% of cellulose [2]; thus, considered as the potential source of nanocellulose, such as cellulose nanocrystals (CNCs) and cellulose nanofibers (CNFs). CNCs and CNFs are different in terms of their shape, size, and composition. CNCs consist of the more crystalline region and have a smaller aspect ratio than CNFs [3]. CNFs have higher strength and modulus than CNCs at the same concentration of nanocellulose [4]. Isolated cellulose fibers and their derivatives have attracted attention for their applications ranging from paper, packaging, sensor, water purification, textile to biomedical devices and drug delivery, due to their advantageous properties such as low density, high surface area, and good mechanical strength [5–11].

Although nanocellulose spark excitement due to several significant merits desirable for various applications, it is often challenging to separate cellulose fibers from plant cells due to its complex structure. Cellulose fibers are mainly bundled up in hemicellulose and lignin, which have adverse effects

on the mechanical separation [12]. The pretreatment method is subjected to fiber sources before the mechanical process to improve the fibrillation. A number of pretreatment methods have been reported for the delignification of biomass, including physical, biological, chemical (Kraft soda, ionic liquids, acid, and alkaline hydrolysis) and combined methods (steam and ammonia fiber explosion) [13–19]. Indeed, each method has its advantages and disadvantages; for example, physical pretreatment such as grinding and milling requires fewer chemicals but consumes high energy, particularly on large scale production [20], while the biological method selectively degrades lignin and hemicellulose, but the rate of hydrolysis is slow and takes a longer time (more than a week) [19–21]. The chemical method is an extensively studied pretreatment technique. For instance, the Kraft process is the most used method in the paper and pulp industry. However, it produces a large number of harmful chemicals, such as hydrogen sulfide [22]. Dilute acid pretreatment can efficiently remove hemicellulose but is corrosive to equipment and creates environmental pollutions [23]. Alkali-based pretreatment is more amenable to enzymatic hydrolysis because it selectively removes lignin and limits the degradation of carbohydrates compared to other chemical methods [24]. This alkaline pretreatment method includes sodium hydroxide, lime, ammonia, and alkaline hydrogen peroxide (AHP) [24,25]. Among alkali-based pretreatments, hydrogen peroxide is extensively used in the pulp and paper industry to bleach and enhance the pulp brightness. The use of hydrogen peroxide generates hydroperoxyl anion at alkaline pH (pH 11.5), which is responsible for dissolving lignin and hemicellulose [26]. Several researchers have contributed to the development of AHP pretreatment for enhancing enzymatic hydrolysis of lignocellulose feedstocks [25,27–29]. For example, Su et al. fractionated lignin and hemicellulose from corncobs with removal ratio of 75.4% and 38.7%, respectively, after 6 h of treatment with AHP [29]. Recently, our team also used AHP hydrolysis and successfully extracted cellulose from various cover crops [30]. After the pretreatment process, CNCs are usually obtained from acid hydrolysis [31].

CNFs are prepared by mechanical methods such as high-pressure micro fluidization, high-pressure homogenization, grinding, and high-intensity ultrasonication [32]. Ultrasonication in a liquid medium can cause both chemical degradation and mechanical disintegration. During the process, it generates high temperature, pressure, and shear force due to acoustic cavitation, and such an extreme environment promotes a reduction in substantial particle size [33,34]. Our research teams have been using the ultrasonication technique to synthesize nanomaterials from various sources such as $CaCO_3$ nanoparticles from eggshells and developed nanoporous MoS_2 nanosheet [34,35]. It is a facial and versatile synthetic tool for nanomaterials that are often unavailable by conventional methods [15]. The ultrasonication method is widely used in CNF preparations from plant biomass and has become a more convenient and emerging approach over the years as a green process [21,36,37]. Feng et al. developed a fine thread-like individual structure of CNFs from pretreated SCB with a steam explosion and alkali-hydrothermal catalysis in combination with 30% H_2O_2 and ultrasonication [12]. Similarly, Khawas et al. isolated crystalline CNFs from the banana peel, pretreated in different chemicals such as NaOH (20%), KOH (5%) $NaClO_3$ (1%) and H_2SO_4 (1%) followed by ultrasonication [38]. Though above-mentioned studies isolated CNF and also considered the environmentally friendly ultrasonication-assisted method, further simplification of processing steps with minimal chemical use is of increasing interest in CNF preparation from plant biomass.

Conversely, film fabrication from CNC/CNF alone is an ongoing challenge due to the lack of common solvents for its dissolution. Available solvents such as ionic liquids are considered as green and efficient but expensive [39]. Other solvents such as NaOH/urea, LiOH/urea, and $ZnCl_2$ solutions are considered facile routes for cellulose dissolution but require further purification steps, which could be detrimental in public health and environmental condition. For example, Salvaggio et al. demonstrated that high exposure to $ZnCl_2$ to aquatic organisms (Zebrafish) causes potential teratogenic effects [40]. Contrary, compression-molding in a hot press is an alternative method to develop high-strength nanocellulose films or sheets from wet cellulose [41,42]. Pintiaux et al. developed a high tensile strength (~22.4 MPa), smooth, plastic-like surface without any additive from commercial α-cellulose using compression-molding in a hot press [43]. It is desirable to formulate environmentally friendly

approaches to utilize and apply cellulose and its derivatives in a wider area. Thus, our study is targeted to simplify the CNF extraction as well as preparation of high-strength glycerol-modified films by minimizing the uses of chemicals and operational approaches. Addition of glycerol in cellulose solution promotes the cellulose-glycerol interaction, reduces brittleness, and increases flexibility [44]. Glycerol is approved for human consumption and also used as a cross-linker for biopolymers [45].

We report here a straightforward, two-step process, yet an effective and environmentally friendly cavitation-based method to extract CNF from agro-residue sugarcane bagasse and develop CNF films. This study was designed to extract CNF in two simple steps: alkaline hydrogen peroxide (AHP) pretreatment, followed by ultrasonication. We used a lower limit of ultrasound frequency (20 kHz) to disintegrate pretreated cellulose into CNF under different degrees of ultrasonication, 1 h, 2 h, and 3 h, herein referred to as CNF-US1, CNF-US2, and CNF-US3, respectively, and determine optimum ultrasonication time. As-obtained CNF suspension was directly used to fabricate glycerol-modified CNF film using hot press and solution casting methods without using harsh chemicals. Furthermore, the properties of extracted CNF and the developed films were evaluated. The characteristics of the extracted CNF was also compared with commercially available nanocellulose.

2. Materials and Methods

2.1. Materials

The sugarcane bagasse (SCB) was obtained from George Washington Carver Agricultural Experimental Station, Tuskegee University, Tuskegee, AL. Obtained SCB was washed thoroughly with deionized water and dried in an oven at 60 °C for 24 h. The bagasse was then cut into small pieces of 1 to 2 cm, pulverized into a fine powder (Supplementary Materials, Figure S1), sieved through 250 µm diameter mesh, and then stored in a desiccator for further use. Ethanol (99.5%), hydrogen peroxide (ACS reagent 30% containing inhibitors), and sodium hydroxide were purchased from Sigma-Aldrich Co., St. Louis, USA. Two types of commercial nanocellulose (cellulose nanofibers (CNF) spray dry (Lot#U37), and cellulose nanocrystal (CNC) spray dry-sodium form (Lot#2015-FPL-CNC-077)) were purchased from University of Maine, Process Development Center, Maine, USA. Commercial nanocellulose was used in this study to track and compare the structural properties of our isolated cellulose fiber. Alkaline hydrogen peroxide (AHP) solution was prepared by adding 1 N NaOH in 3% H_2O_2 solution and adjusted to a pH of 11.5.

2.2. Alkaline Hydrogen Peroxide (AHP Hydrolysis)

The AHP hydrolysis was performed to remove hemicellulose and lignin from SCB with a slight modification of the method described by Sun et al. [2]. In this process, the pulverized dry powder was continuously stirred in AHP solution in a water bath using a magnetic stirrer at 150 rpm at ~40 °C for 4 h. Throughout the AHP hydrolysis, the pH of the solution was periodically adjusted (~11.5). It is because H_2O_2 dissociates into reactive radicals and dissolves lignin of the reaction mixture [26]. The final liquid-to-sample ratio was 150 mL/g. After the pulping process, the pH of the mixture was adjusted neutral with the addition of 2 N H_2SO_4. The insoluble residue was collected under vacuum filtration and washed with deionized water (3 times) to remove all the soluble materials. The remaining white cellulose pulp residue was dried and labeled as "*cellulose*".

2.3. Extraction of CNF Using Ultrasonication

The AHP-hydrolyzed cellulose (0.5% *W*/*V*) was ultrasonically irradiated at 1 h, 2 h, and 3 h in 1% H_2O_2 solution with a low-frequency (20 kHz) ultrasound processor (Sonics and Materials Inc., Vibra Cell, VC-750, USA) in an ice bath support in order to avoid overheating of the samples. Hydrogen peroxide was used to dissolve residual lignin and hemicellulose. The processor was equipped with a cylindrical titanium alloy probe tip of diameter 13 mm. Other conditions of the

processor were the output power, 750 W, and an amplitude of 70% with 15 s on and 5 s off cycle. The actual energy dissipated into the liquid was calculated from the following equation:

$$W = mC_p\ (\Delta T/dt) \quad (1)$$

where W is power, m is the mass of the solution taken in 'kg', Cp is the specific heat of liquid at constant pressure (4.180 J/kg/ K), ΔT is the change in initial and final temperature in 'K', and dt is the reaction time in 'S' [46]. The temperature difference during the course of the reaction was observed ~30 K and the corresponding power disseminated was ~2.1 W. After completion of sonication times, few drops of 2 N H_2SO_4 were added to the suspension (pH 5.0) and vigorously mixed using vortex for 2 min to prevent the agglomeration of disintegrated fibers. The addition of H_2SO_4 after ultrasonication prevents possible corrosion of the equipment. Obtained colloidal suspensions were labeled as CNF-US1, CNF-US2, and CNF-US3 for cellulose sonicated at 1 h, 2 h, and 3 h, respectively. A set of the sonicated samples were freeze-dried (SP Scientific, VirTis Bench Top Pro, USA) at −78 °C for 72 h to determine structural properties, while another set was directly used as a suspension for film preparation and evaluated physical and chemical properties of the films. The sample processing steps and obtained results in each stage of treatment are available in supporting files (Supplementary Materials, Figure S1). Fiber samples from each stage of CNF extractions were analyzed using the following characterization techniques.

2.4. X-ray Diffraction (XRD)

The X-ray diffraction (XRD) patterns were recorded with a wide-angle X-ray diffractometer (Rigaku DMAX 2100, containing monochromatic CuK α radiation (λ = 0.15418 nm). The accelerating voltage was 40 kV, the current was 30 mA, and the scanning range between 5° and 50° angle with the scan rate of 2°/min. The crystallinity intensity was determined by the peak height method. The XRD data were analyzed using MDI JADE software (Version 7.8.1, ©MDI). In conjunction, the crystallinity of the samples was compared with the Raman spectroscopy.

2.5. Raman Spectroscopy

Raman spectroscopy (DXR, Thermo Scientific, MA, USA) equipped with 780 nm (3.0 mW power) wavelength laser was used to understand the change in the chemical structure of the samples after each successive treatment. The data acquisition was carried out in a range of 25–3500 cm^{-1} using OMNIC software. The intensity ratio (I_{380}/I_{1096}) was determined, and Raman crystallinity (index of crystallinity—IC) was calculated using the following equation [47].

$$IC = [(\frac{I_{380}}{I_{1096}}) - 0.0286]/0.0065 \quad (2)$$

2.6. Field-Emission Scanning Electron Microscopy (FE-SEM)

Surface morphology was evaluated using a field emission-scanning electron microscope (a JEM-JSM-7200F, Japan). During the process, samples were mounted on conductive adhesive carbon tape and sputtered with gold/palladium target for 5 min, and plasma discharge current was maintained below 10 milliamperes [48].

2.7. Thermal Gravimetric Analysis (TGA)

The thermal property was evaluated using a thermal gravimetric analyzer (TGA Q500 series, TA instrument, DE, USA). Samples were analyzed under a nitrogen atmosphere to prevent thermoxidative process from 30 to 600 °C at the constant heating rate of 5 °C/min.

2.8. Attenuated Total Reflectance Fourier Transform Infrared Spectroscopy (ATR-FTIR)

The chemical properties of the CNF films were determined using attenuated total reflectance-FTIR (Nicolet, Nexus model 670/870, Thermo Electron Corporation, WI, USA) at room temperature. The spectra were recorded between 650 and 4000 cm^{-1} with a resolution of 4 cm^{-1}, and total scans were 32 per sample. Initial background spectra were taken and subtracted from the sample measurement.

2.9. CNF Films Preparation

Obtained gel-like suspension of CNFs from ultrasonication was used to prepare films using two methods without further purification: 1. hot press and 2. solution casting. In both methods, consistent volume (40 mL of 0.5% *W*/*V*) of CNF suspension was used. In the hot press, CNF suspensions were vacuum filtered using Whatman filter paper, sandwiched in the layer of a hydrogel in filter papers, and conditioned in the oven for 1 h at 100 ± 5 °C to evaporate excess water. The films were gently peeled and sandwiched in new set of filter paper and hot pressed (CARVER®, model number 4386, Carver, Inc., IN, USA) using ~10,000 to 12,000 lbs pressure at 105 °C for 15 min. Whereas, in the solution casting method, CNF suspension was first centrifuged at 5000 rpm for 10 min, decanted water andresuspended into ethanol (100%) to decrease the evaporation time of films, and centrifuged again at 1000 rpm for 1 min to avoid air bubbles. Native cellulose film is brittle; therefore, cellulose was modified with the addition of glycerol (30% of the dry weight of CNF) into CNF suspension. The modified CNF solution was gently poured onto a polyethylene Petri dish (90 mm diameter) and left for atmospheric evaporation at room temperature for ~48 h. All the CNF films were conditioned before characterization in an environmental chamber at 30 °C and 55% relative humidity for 24 h.

2.10. Mechanical Properties Testing

The mechanical properties of CNF films were analyzed using a texture analyzer (TA-HD plus, Stable Micro Systems, UK) with 50 kg load cell. The tensile test was performed according to ASTM D882-02. The tests were conducted with an extension rate of 10 mm/min at room temperature. The initial gap of the sample and grip was 40 mm (sample size: thickness 0.12 to 0.16 mm, width 10 mm, and length 75 mm), five specimens from each sample were tested. The Young's modulus of the films was determined from the linear fitted trend line to the initial steep sections of the typical stress-strain curve.

3. Results and Discussion

3.1. Effects of AHP Hydrolysis and Ultrasonication on Cellulose

CNFs were extracted from SCB using a two-step method as shown in Figure 1. The first step involves alkaline hydrogen peroxide (AHP) hydrolysis, and this process changed brown sugarcane bagasse-raw into the cellulose-rich creamy white pulp. Alkaline conditions break the intermolecular ester bond between lignin and carbohydrate [49]. The highly reactive -OH radicals formed during the degradation of H_2O_2 reacts rapidly with lignin into low-molecular-weight water-soluble oxidation products responsible for lignin dissolution [26]. The second step involves the ultrasonication of the cellulose. This step was performed to optimize the ultrasonication time varying from 1 h to 3 h and its effect on the composition and structural properties of the fibers. Composition analysis and quantification were performed using the NREL method [50]. Sugarcane bagasse-raw contents cellulose, hemicellulose, and lignin, approximately 39%, 20%, and 33%, respectively. Cellulose (glucan) concentration found from cellulose, 1 h, 2 h, and 3 h was approximately 67%, 86.1%, 92.5%, and 92.7%, respectively. Lignin concentration was approximately 13%, 3.5%, 1.5%, and 1.4%, respectively. The hemicellulose was not detected (xylan) or there was a very low amount after AHP treatments; these results are underway and will be published shortly (Supplementary Materials, Table S1). The above results indicated that the concentration of cellulose is increased while the concentration of lignin is decreased after the ultrasonic-assisted method. It indicated that the applied methods removed non-cellulosic

contents. It might be due to the disruption of ether bonds between lignin and hemicellulose [51]. However, there was not much difference in lignocellulosic composition values at 2 h compared to 3 h.

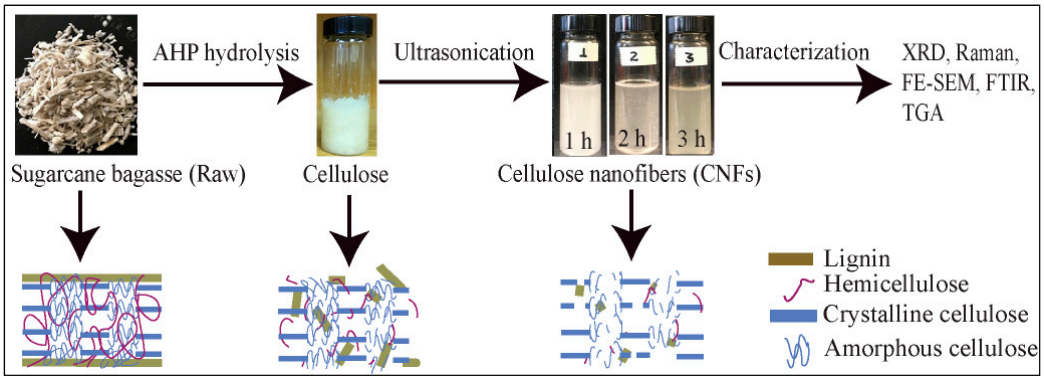

Figure 1. The two-step extraction process of cellulose nanofibers from sugarcane bagasse (top) with gel-like cellulose suspension after ultrasonication, and schematic illustration showing progressive removal of non-cellulosic constituents and formation cellulose nanofibers during the process (bottom).

Hence, the ultrasonication time of 2 h was considered as an optimum time for cellulose extraction. Ultrasonication of cellulose was observed to disintegrate bulk cellulose into gel-like suspension and most likely to be CNFs (see Figure 1). Ultrasound dissociated H_2O_2 into -hydroxyl radicals through chain reactions; these react with lignin and convert them into simple phenol [52]. In conjunction, ultrasonication produces cavitation bubbles, which acts as a local hotspot, as the bubbles collapse, produce strong shock waves creating exceptionally high temperatures, pressures, and massive shear force, upon strike on bulk materials disintegrated into nanoparticles [34]. Thus, the synergistic effects of H_2O_2 and the ultrasonication process at low temperatures might be an effective alternative to generate CNF. In the schematic illustration showing progressive removal of majority of the non-cellulosic components, there might be a small amount of lignin and hemicellulose even after AHP pretreatment (see Figure 1). The presence of lignin and hemicellulose was also detected by FTIR in our study after the pretreatment (Supplementary Materials, Figure S2). It is difficult to completely remove lignin and hemicellulose from the plant biomass by alkaline pretreatment due to its complex structure of plant biomass. Our results are consistent with other researches. The alkaline or organic solvent pretreatment method removed 91% lignin, and 89.1% of the hemicellulose from pine sawdust where AHP pretreatment delignified more than 80% from corn stover [25,53]. Next, we characterized as-obtained gel-like cellulose suspensions and analyzed its structural, morphological, chemical, thermal, and mechanical properties, which is discussed below.

3.2. Structural Characterization of Extracted Cellulose and CNF

XRD pattern of SCB-raw (sugarcane bagasse-raw), cellulose, ultrasonicated cellulose, and commercial cellulose is shown in Figure 2. The crystalline index (CrI) of samples was calculated by Segal method [54], and the results are tabulated in Supplementary Materials, Table S2. The percentage of the CrI of SCB-raw, cellulose (AHP-hydrolyzed), ultrasonication at 1 h, 2 h, 3 h, commercial CNF, and commercial CNC were 35.1%, 45.4%, 52.7%, 57.7%, 61.6%, 66.7%, and 55.9%, respectively. The intensity and peaks were more defined and sharpened with the increase of ultrasonication time. The fiber crystallinity of 2 h and 3 h were slightly different, but we selected 2 h as an optimum time for CNF production in our study. The main 2θ diffractions were close to 16.5°, and 22.2° and are associated with the crystalline cellulose. The XRD data indicated that the crystalline morphology of cellulose did not change during treatment, but the crystallinity of the fiber was improved. Fiber crystallinity from 3 h ultrasonication was ~61.6%, which represents over 30% of that of SCB-raw. Our results are similar to the findings reported by Kumar et al. from acid-treated sugarcane bagasse, in which sugarcane bagasse, purified cellulose, and cellulose nanocrystal were 35.6%, 63.5%, and 72.5%, respectively [16].

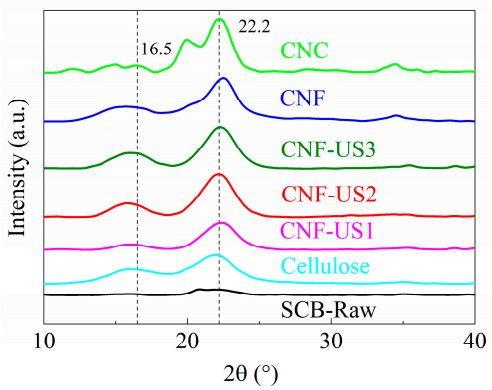

Figure 2. X-ray diffraction patterns of sugarcane bagasse-raw (SCB-raw), AHP-treated (cellulose), ultrasonication for 1 h, 2 h, and 3 h (CNF-US1, CNF-US2, and CNF-US3), and commercial celluloses (CNF and CNC).

A comparison of the Raman spectra of samples is shown in Figure 3. The calculated crystallinity indices from the ratio of I_{380} and I_{1096} were obtained from sugarcane bagasse-raw (SCB-raw), CNF-US2, commercial CNF, and commercial CNC at 38.1%, 61.2%, 55.3%, and 76.6%, respectively. In terms of crystallinity, observed results from the Raman analysis are coherent with the XRD results. The peaks are sharper in commercial CNC as compared to commercial CNF as well as ultrasonicated CNF (CNF-US2) from sugarcane. This observation could be due to the higher percentage of crystallinity in CNC. Raman spectroscopy provides information on structural orientation and investigates the chemical mapping of lignocellulosic biomass [55]. In conjunction, the crystallinity of the extracted cellulose can be estimated and compared with XRD [56]. Therefore, Raman spectroscopy was conducted as a supplementary method for XRD in our study.

Prominent peaks from commercial and ultrasonicated samples were observed at 380, 900, 1061, 1121, 1380, 1460, and 2890 cm^{-1}. The assigned Raman peaks for cellulose in our study are in agreement with the previously reported peaks for cellulose from biomass [57,58]. Additionally, there were no, or only minor peaks recorded between 1500 and 2800 cm^{-1} spectral range both in commercial and ultrasonicated samples, which could be due to the removal of lignin. The dominant peaks for lignin in the plant biomass samples were suggested at around 1600 cm^{-1} [56,59]. The high-intensity peaks were recorded at 1602 and 1631 cm^{-1} only in SCB-raw. These results strongly indicated that the lignin was successfully removed from sugarcane bagasse. These findings were further supported by FTIR results (Supplementary Materials, Figure S3). Ultrasound-treated samples followed a similar pattern with commercial cellulose nanofiber (CNF); therefore, only CNF were compared in thermal analysis.

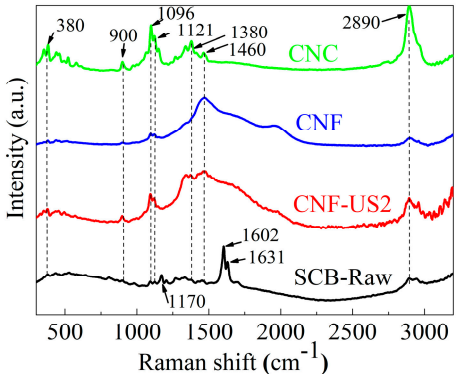

Figure 3. Comparison of Raman spectra of sugarcane bagasse-raw (SCB-raw), ultrasonication for 2 h (CNF-US2) and commercial celluloses (CNF and CNC).

3.3. Morphological Characterization of the Raw SCB and CNFs

FE-SEM was conducted to analyze the changes in surface morphology of CNF due to ultrasonication. Figure 4a–d show FE-SEM images of different samples, SCB-raw, and ultrasonication at 1 h, 2 h, and 3 h. A definite change in the morphological structure of the cellulose fibers occurred upon ultrasonication. Figure 4a shows the surface morphology of SCB-raw fibers regularly arranged, covered with residual materials, and bound tightly together in a bundle, which could be due to the presence of the waxy layer and intact lignocelluloses components [60,61]. A remarkable effect on the fiber morphology has occurred in ultrasonicated samples compared to SCB-raw. For example, fibers are detached from the bundle and produced an entangled structure with a fiber diameter less than 100 nm (see Figure 4b–d). It might be due to the synergistic effects of H_2O_2 and ultrasonication. Cellulose nanofibers consist of a bundle of stretched cellulose chain molecules with long, web-like, and highly entangled nanofibers of approximately 6–100 nm size generally produced by mechanical pressure [4]. The intertwined fiber structure might be due to ultrasonication that increases the surface area of fibers and leads to strengthening intermolecular hydrogen bonding and hydrophilic interaction between cellulose molecules [12,16].

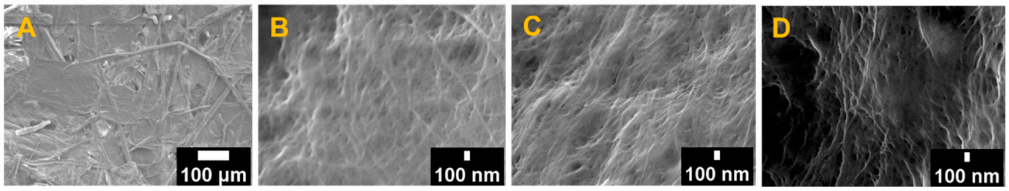

Figure 4. FE-SEM images: (**a**) SCB-raw; (**b**) Ultrasonication for 1 h (CNF-US1); (**c**) Ultrasonication for 2 h (CNF-US2) and (**d**) Ultrasonication for 3 h (CNF-US3).

Finally, the thermal stability of the samples was compared, as shown in Figure 5a,b (Supplementary Materials, Table S3). All samples showed a slight weight loss (<0.5%) at lower temperatures starting around 35 °C; it is due to evaporation of loosely bound water. The initial weight loss at around 100 to 120 °C was around 10%; it is ascribed to the vaporization of water because of the hydrophilic character of cellulose fiber. In this temperature range, intermolecular H-bonded water and absorbed water is evaporated [16]. There was no remarkable weight changed around 150 °C except SCB-raw; it may be due to the absence of volatile and low molecular weight compounds in ultrasonicated samples. However, the onset temperature of ultrasonicated samples was initiated at a lower temperature (~190 °C) compared to raw (225 °C) and commercial CNF (205 °C). Increase in onset temperature in the SCB-raw sample could be linked to its chemical composition and cross-linked with a heavy molecular weight of lignin, which facilitated to improve thermal stability and thus difficult to decompose at a lower temperature [62]. Higher crystallinity produces a fast heat transferability and decomposes earlier [63]. However, in our study, onset temperature was increased with increased crystallinity. Lower onset temperature in the ultrasonicated samples might be due to short cellulose chain and small particle size. The high surface area of CNF results in the formation of free-end-chains on the surface, which facilitated to decompose quickly at the lower temperature [2,34]. The high surface area plays a significant role in diminishing thermal stability due to the increased exposure to heat surface [63].

The onset and decomposition temperature of all the analyzed samples are presented in Table 1 The DTG curve (Figure 5b) revealed that there were differences in the decomposition temperature among samples. Interestingly, significant weight loss of ~35% was observed from 300 to 350 °C with an SCB-raw, whereas only ~10% weight loss was observed with ultrasonicated samples in the same temperature range. It might be due to the presence of lignin and hemicellulose in the SCB-raw sample. This result was further supported by a prominent shoulder around 290 °C along with a broad peak from 200 to 500 °C in the DTG's curve (See Figure 5b), indicating that the raw sample contained lignin and hemicellulose. The aromatic ring structure of lignin resulted in its wide degradation temperature range of 250 to 700 °C [12]. However, with AHP hydrolysis followed by ultrasonication, DTG curves showed

sharper peaks in the temperature range between 250 and 300 °C without a shoulder. It might be due to the removal of lignin and hemicellulose and also might be due to an increase in the crystallinity of the fibers, as evidenced by XRD measurements. Therefore, the percentage of weight loss in CNF-US2 and CNF-US3 was less (<5%), in the temperature range of 300 to 350 °C.

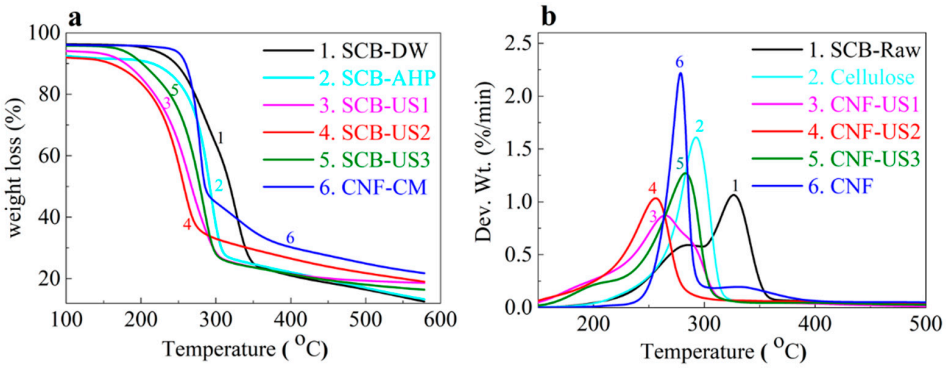

Figure 5. (**a**) TGA curves and (**b**) DTG graphs of sugarcane bagasse-raw (SCB-raw), AHP-treated (cellulose), CNF prepared using ultrasonication for 1 h, 2 h, and 3 h (CNF-US1, CNF-US2, and CNF-US3), and commercial cellulose nanofiber (CNF).

Table 1. Onset and maximum decomposition temperature of SCB-raw, AHP-treated (cellulose), ultrasonication at 1 h, 2 h, and 3 h (CNF-US1, CNF-US2, CNF-US3), and commercial cellulose nanofibers (CNF).

Temp. (°C)	SCB-raw	Cellulose	CNF-US1	CNF-US2	CNF-US3	CNF
Onset	225	195	190	195	205	220
Max. dec.	325	290	255	265	280	280

3.4. CNF Film Preparation and Mechanical Property Analysis

A representative stress-strain curve of CNF films using hot press and solution casting is shown in Figure 6, and film preparation process including digital images of as produced films are shown in Figure S3 (see Supplementary Materials, Figure S3). Table 2 shows Young's modulus, tensile strength, and elongation at break of CNF films. Regardless of the film's fabrication methods, the tensile strength was increased with increasing ultrasonication time. Young's modulus was increased more than ten times in all film produced from the hot press as compared to solution casting. Tensile strength also increased in films produced from the hot press; maximum improvement in tensile strength in hot press compared to solution casting was exhibited by films produced from CNF-US2, and the strength value (25 MPa) was eight-fold higher than value (3.5 MPa) from solution casting method (see Table 2).

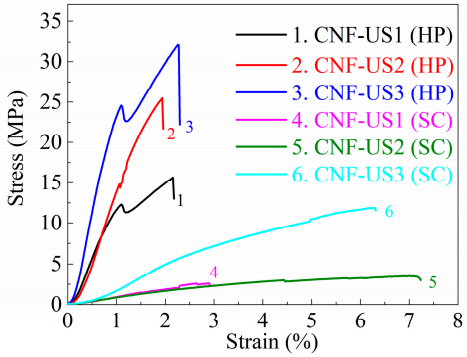

Figure 6. The stress-strain curve of films using a hot press (HP) and solution casting (SC).

Table 2. Mechanical properties of the CNF film produce from the suspension of CNF-US1, CNF-US2, and CNF-US 1, by hot press and solution casting.

	Young's Modulus (GPa)	Tensile Strength (MPa)	Elongation (%)
Hot Press (HP)			
CNF-US1	1.7 ± 0.7	15.4 ± 3	1.7 ± 0.7
CNF-US2	1.7 ± 0.5	25.0 ± 2	1.7 ± 0.5
CNF-US3	2.3 ± 0.5	31.0 ± 3	2.0 ± 0.7
Solution Casting (SC)			
CNF-US1	0.1 ± 0.03	2.5 ± 0.5	3.3 ± 0.3
CNF-US2	0.1 ± 0.02	3.5 ± 0.1	6.7 ± 1
CNF-US3	0.2 ± 0.04	10.2 ± 2	6 ± 1.5

Improvement in tensile property might be the result of enhanced contact area between nanoscale CNF building blocks that facilitated: homogeneous dispersion, higher packaging density, and more overlapping between neighboring fibers. The mechanical properties of the cellulose films have a strong dependence on the size of the CNF. The smaller size of CNF could result in high strength films [64]. In our study, the mechanical properties of the films were increased with increasing ultrasonication time. It could be due to decrease in the size of the cellulose fibers during ultrasonication. Reduction in size increases the surface area that leads to an increase in hydrogen bonding [12]. Ghaderi et al. reported a similar result in which tensile strength is increased in almost twelve folds by converting bagasse fiber into nanofiber using a hot press [65]. Increased tensile strength of films in our study might be due to hydroxyl group interaction between glycerol and CNF. Plasticizer might have caused the formation of new hydrogen bonds networks; thus, changing the properties of the films [31]. Besides, the crystallinity of the fibers increased with ultrasonication; this might be another factor responsible for increasing the strength of films. It is reported that crystallinity is directly proportional to the stiffness and rigidity of the materials [66]. Similarly, the mechanical properties of the cellulose films are influenced by the moisture content. The hot press was operated at temperature (~105 °C); thus, it could have resulted in less moisture in between the CNF matrix than the solution casting method. The water can weaken the average hydrogen bonding in the cellulose structure by the process of exchange from cellulose/cellulose to cellulose/water hydrogen bonds. An increase in water content has been reported to decrease tensile strength and Young's modulus [67]. In our study, films produced by hot press increased the mechanical properties of the films in a short time (15 min) compared to solution casting (48 h). Thus, it is assumed that the ultrasonically extracted CNF modified with glycerol could be developed into sustainable and environmentally friendly high-strength cellulose film by hot press.

We also performed ATR-FTIR measurements on CNF films to understand the effect of sonicated time and film preparation method (hot press and solution casting) on the inter and intra-molecular interaction (See Figure 7). With an increase in ultrasonic time, spectrum intensity is increased, and the shift of the -OH group has occurred, especially at 1061 cm^{-1} (See Figure 7). These shifts indicate that the decrease in the degree of free O-H might have resulted from better dispersion of CNFs and subsequent increase in interfacial adhesive bonding. It is because ultrasonication increases the surface area of fibers by reducing the size that leads to an increase in hydrogen bonding. The crystalline structure of cellulose is due to hydrogen bond interaction and Vander Walls force to the adjacent molecules [68]. Crystallinity is directly proportional to the stiffness and rigidity of the materials [69]. Therefore, crystallinity and the size of the cellulose play an essential role in the mechanical strength of the films. The dominant broad peaks around 3000 to 3500 cm^{-1} were due to O-H and C-H stretching of the OH- and CH- group in cellulose molecules, and a sharp band at 2900 cm^{-1} represents C-H stretching [69]. A peak at 1645 cm^{-1} on spectra of CNF-US1 (HP) represents the vibration of acetyl and uronic ester groups of hemicelluloses or ester linkage of the carboxylic group of ferulic and *p*-coumaric acids of lignin, and this peak was not observed or there was low intensity with increased ultrasonic time (See Figure 7). The most significant absorption band at 1061 cm^{-1} associated with the β-glycosidic

linkages between glucose units in cellulose, which was increased progressively with increase in the ultrasonication time; a similar peak was reported by Gierlinger et al. [70]. The spectral profiles and relative intensities of the bands were similar in both hot pressed and solution cast films, indicating similar chemical structures. Therefore, only representative sample CNF-US2 (SC) from solution casting was presented in Figure 7.

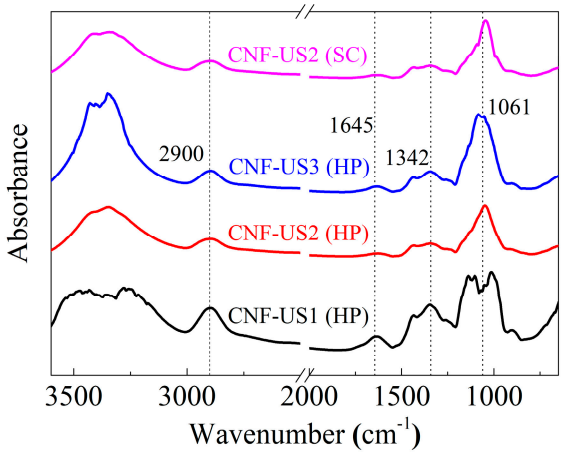

Figure 7. ATR-FTIR spectra of films prepared from 1 h, 2 h, and 3 h ultrasonicated CNF as CNF-US1 (HP), CNF-US2 (HP), CNF-US3 (HP) and solution casting as CNF-US2 (SC).

4. Conclusions

We report extraction of CNF from agricultural waste sugarcane bagasse using a low-frequency ultrasonication method. This straightforward method was able to produce highly crystalline cellulose fibers, and the properties of our CNF were found similar to those of commercial CNF. Further, we fabricated films of CNF in an organic solvent-free medium. Our results demonstrated that hot press is a more prevailing method to produce high strength CNF films than solution casting. The elasticity of the films was reduced, but extracted CNF could be used as a potential polymer reinforcement for composite materials. We note that our method for extracting CNF and making films, by its simplicity, could be an efficient approach in broad applications such as a hydrogel, gas sensors, and packaging materials development, which will be the subject of future studies. Finally, the availability of abundant agricultural residues could be the competent feedstocks to generate sustainable and value-added biopolymers, such as nanoscale cellulose and dissolving pulp, for industrial applications to overcome excessive dependence on synthetic polymers.

Supplementary Materials: The following are available online at http://www.mdpi.com/2071-1050/12/15/6015/s1, Figure S1: The transformation process of sugarcane bagasse to cellulose nanofiber: 1. Sugarcane bagasse-raw with a pulverized fine powder, 2. AHP-hydrolyzed pulp cellulose (below) and dried powder (above) and 3. Ultrasonication gel-like CNF at 1 to 3 h (below) and freeze-dried fibers (above), Figure S2: FTIR spectrum: a. A comparative spectrum of SCB-raw, CNF obtained at 1 h, 2 h and 3 h sonic (CNF-US1, CNF-US2, and CNF-US3), and commercial cellulose (CNF), b. Magnified spectrum of all the samples and highlighted (light yellow) box indicates lignin or hemicellulose region, SCB-raw (black spectra) have prominent peaks, Table S1: Composition analysis of sugarcane bagasse, cellulose, and ultrasonicated fibers at 1 h, 2 h, and 3 h, Table S2: Crystallinity property of raw (SCB-raw), AHP-treated (cellulose), ultrasonication at 1 h, 2 h, and 3 h (CNF-US1, CNF-US2 and CNF-US3) and commercial cellulose (CNC and CNF), Table S3: Percentage residue (% weight loss) at different temperatures for raw (SCB-raw), AHP-treated (cellulose), ultrasonication at 1 h, 2 h, and 3 h (CNF-US1, CNF-US2, and CNF-US3) and commercial cellulose (CNF).

Author Contributions: N.S. designed, visualized, and performed the experiments, investigated, analyzed the data, and prepared the original manuscript. B.M. and V.K.R. conceived the study, reviewed, edited the manuscript, and supervised the research. B.S. assisted with XRD measurements, reviewed, and co-wrote the article. All authors have read and agreed to the published version of the manuscript.

Funding: This research work was supported by the grant awarded from the United States Department of Agriculture (USDA)/National Institute of Food and Agriculture (NIFA) (grant no. 2015-38821-24376). The authors

also would like to acknowledge the financial support of NSF-RISE no. 1459007, NSF-CREST no. 1735971, and NSF-MRI-1531934 grants.

Conflicts of Interest: The authors declare no conflict of interest.

References

1. Biswas, A.; Saha, B.C.; Lawton, J.W.; Shogren, R.L.; Willett, J.L. Process for obtaining cellulose acetate from agricultural by-products. *Carbohydr. Polym.* **2006**, *64*, 134–137. [CrossRef]
2. Sun, J.X.; Sun, X.F.; Zhao, H.; Sun, R.C. Isolation and characterization of cellulose from sugarcane bagasse. *Polym. Degrad. Stab.* **2004**, *84*, 331–339. [CrossRef]
3. Salas, C.; Nypelö, T.; Rodriguez-Abreu, C.; Carrillo, C.; Rojas, O.J. Nanocellulose properties and applications in colloids and interfaces. *Curr. Opin. Colloid Interface Sci.* **2014**, *19*, 383–396. [CrossRef]
4. Xu, X.; Liu, F.; Jiang, L.; Zhu, J.Y.; Haagenson, D.; Wiesenborn, D.P. Cellulose nanocrystals vs. cellulose nanofibrils: A comparative study on their microstructures and effects as polymer reinforcing agents. *ACS Appl. Mat. Interfaces* **2013**, *5*, 2999–3009. [CrossRef] [PubMed]
5. Khan, A.; Wen, Y.; Huq, T.; Ni, Y. Cellulosic nanomaterials in food and nutraceutical applications: A review. *J. Agric. Food Chem.* **2018**, *66*, 8–19. [CrossRef] [PubMed]
6. Rhim, J.W.; Kim, Y.T. *Biopolymer-Based Composite Packaging Materials with Nanoparticles*; Academic Press: Cambridge, MA, USA, 2013. [CrossRef]
7. Yadav, S.K. *Nanoscale Materials in Targeted Drug Delivery, Theragnosis and Tissue Regeneration*; Springer: Berlin, Germany, 2016. [CrossRef]
8. Ummartyotin, S.; Manuspiya, H. A critical review on cellulose: From fundamental to an approach on sensor technology. *Renew. Sustain. Energy Rev.* **2015**, *41*, 402–412. [CrossRef]
9. Orelma, H.; Hokkanen, A.; Leppänen, I.; Kammiovirta, K.; Kapulainen, M.; Harlin, A. Optical cellulose fiber made from regenerated cellulose and cellulose acetate for water sensor applications. *Cellulose* **2020**, *27*, 1543–1553. [CrossRef]
10. Khan, A.; Abas, Z.; Kim, H.S.; Kim, J. Recent progress on cellulose-based electro-active paper, its hybrid nanocomposites and applications. *Sensors* **2016**, *16*, 1172. [CrossRef]
11. Voisin, H.; Bergström, L.; Liu, P.; Mathew, A. Nanocellulose-based materials for water purification. *Nanomaterials* **2017**, *7*, 57. [CrossRef]
12. Feng, Y.H.; Cheng, T.Y.; Yang, W.G.; Ma, P.T.; He, H.Z.; Yin, X.C.; Yu, X.X. Characteristics and environmentally friendly extraction of cellulose nanofibrils from sugarcane bagasse. *Ind. Crops Prod.* **2018**, *111*, 285–291. [CrossRef]
13. Perrone, O.M.; Colombari, F.M.; Rossi, J.S.; Moretti, M.M.S.; Bordignon, S.E.; Nunes, C.D.C.C.; Gomes, E.; Boscolo, M.; Da-Silva, R. Ozonolysis combined with ultrasound as a pretreatment of sugarcane bagasse: Effect on the enzymatic saccharification and the physical and chemical characteristics of the substrate. *Bioresour. Technol.* **2016**, *218*, 69–76. [CrossRef] [PubMed]
14. Zuluaga, R.; Putaux, J.L.; Cruz, J.; Vélez, J.; Mondragon, I.; Gañán, P. Cellulose microfibrils from banana rachis: Effect of alkaline treatments on structural and morphological features. *Carbohydr. Polym.* **2009**, *76*, 51–59. [CrossRef]
15. Bang, J.H.; Suslick, K.S. Applications of ultrasound to the synthesis of nanostructured materials. *Adv. Mat.* **2010**, *22*, 1039–1059. [CrossRef] [PubMed]
16. Kumar, A.; Singh Negi, Y.; Choudhary, V.; Bhardwaj, N.K. Characterization of cellulose nanocrystals produced by acid-hydrolysis from sugarcane bagasse as agro-waste. *J. Mat. Phys. Chem.* **2014**, *2*, 1–8. [CrossRef]
17. Kim, D. Physico-chemical conversion of lignocellulose: Inhibitor effects and detoxification strategies: A mini review. *Molecules* **2018**, *23*, 309. [CrossRef] [PubMed]
18. Cara, C.; Ruiz, E.; Oliva, J.M.; Sáez, F.; Castro, E. Conversion of olive tree biomass into fermentable sugars by dilute acid pretreatment and enzymatic saccharification. *Bioresour. Technol.* **2008**, *99*, 1869–1876. [CrossRef] [PubMed]
19. Kumar, P.; Barrett, D.M.; Delwiche, M.J.; Stroeve, P. Methods for pretreatment of lignocellulosic biomass for efficient hydrolysis and biofuel production. *Ind. Eng. Chem. Res.* **2009**, *48*, 3713–3729. [CrossRef]

20. Sofla, M.R.K.; Brown, R.J.; Tsuzuki, T.; Rainey, T.J. A Comparison of cellulose nanocrystals and cellulose nanofibres extracted from bagasse using acid and ball milling methods. *Adv. Nat. Sci. Nanosci. Nanotechnol.* **2016**, *7*, 035004. [CrossRef]
21. Hassan, S.S.; Williams, G.A.; Jaiswal, A.K. Emerging technologies for the pretreatment of lignocellulosic biomass. *Bioresour. Technol.* **2018**, *262*, 310–318. [CrossRef]
22. Mathew, A.K.; Abraham, A.; Mallapureddy, K.K.; Sukumaran, R.K. *Lignocellulosic Biorefinery Wastes, or Resources?* Elsevier: Amsterdam, The Netherlands, 2018. [CrossRef]
23. Santucci, B.S.; Bras, J.; Belgacem, M.N.; Curvelo, A.A.D.S.; Pimenta, M.T.B. Evaluation of the effects of chemical composition and refining treatments on the properties of nanofibrillated cellulose films from sugarcane bagasse. *Ind. Crops Prod.* **2016**, *91*, 238–248. [CrossRef]
24. Kim, J.S.; Lee, Y.Y.; Kim, T.H. A review on alkaline pretreatment technology for bioconversion of lignocellulosic biomass. *Bioresour. Technol.* **2015**, *199*, 42–48. [CrossRef] [PubMed]
25. Mittal, A.; Katahira, R.; Donohoe, B.S.; Black, B.A.; Pattathil, S.; Stringer, J.M.; Beckham, G.T. Alkaline peroxide delignification of corn stover. *ACS Sustain. Chem. Eng.* **2017**, *5*, 6310–6321. [CrossRef]
26. Gould, J.M. Studies on the mechanism of alkaline peroxide delignification of agricultural residues. *Biotechnol. Bioeng.* **1985**, *27*, 225–231. [CrossRef] [PubMed]
27. Karagöz, P.; Rocha, I.V.; Özkan, M.; Angelidaki, I. Alkaline peroxide pretreatment of rapeseed straw for enhancing bioethanol production by same vessel saccharification and co-fermentation. *Bioresour. Technol.* **2012**, *104*, 349–357. [CrossRef]
28. Dutra, E.D.; Santos, F.A.; Alencar, B.R.A.; Reis, A.L.S.; de Souza, R.D.F.R.; Aquino, K.A.D.S.; Morais, M.A.; Menezes, R.S.C. Alkaline hydrogen peroxide pretreatment of lignocellulosic biomass: Status and perspectives. *Biomass Convers. Biorefin.* **2018**, *8*, 225–234. [CrossRef]
29. Su, Y.; Du, R.; Guo, H.; Cao, M.; Wu, Q.; Su, R.; Qi, W.; He, Z. Fractional pretreatment of lignocellulose by alkaline hydrogen peroxide: Characterization of its major components. *Food Bioprod. Process.* **2015**, *94*, 322–330. [CrossRef]
30. Shahi, N.; Joshi, G.; Min, B. Potential sustainable biomaterials derived from cover crops. *BioResources* **2020**, *15*, 5641–5652. [CrossRef]
31. Csiszár, E.; Nagy, S. A comparative study on cellulose nanocrystals extracted from bleached cotton and flax and used for casting films with glycerol and sorbitol plasticisers. *Carbohydr. Polym.* **2017**, *174*, 740–749. [CrossRef]
32. Abdul Khalil, H.P.S.; Davoudpour, Y.; Islam, M.N.; Mustapha, A.; Sudesh, K.; Dungani, R.; Jawaid, M. Production and modification of nanofibrillated cellulose using various mechanical processes: A review. *Carbohydr. Polym.* **2014**, *99*, 649–665. [CrossRef]
33. Nakashima, K.; Ebi, Y.; Kubo, M.; Shibasaki-Kitakawa, N.; Yonemoto, T. Pretreatment combining ultrasound and sodium percarbonate under mild conditions for efficient degradation of corn stover. *Ultrason. Sonochem.* **2016**, *29*, 455–460. [CrossRef]
34. Hassan, T.A.; Rangari, V.K.; Rana, R.K.; Jeelani, S. Sonochemical effect on size reduction of $CaCO_3$ nanoparticles derived from waste eggshells. *Ultrason. Sonochem.* **2013**, *20*, 1308–1315. [CrossRef] [PubMed]
35. Wanunu, M.; Sapkota, B. Porous Membranes Comprising Nanosheets and Fabrication Thereof. U.S. Patent 20190039028, 7 February 2019.
36. Patist, A.; Bates, D. Ultrasonic innovations in the food industry: From the laboratory to commercial production. *Innov. Food Sci. Emerg. Technol.* **2008**, *9*, 147–154. [CrossRef]
37. Bundhoo, Z.M.A.; Mohee, R. Ultrasound-assisted biological conversion of biomass and waste materials to biofuels: A review. *Ultrason. Sonochem.* **2018**, *40*, 298–313. [CrossRef] [PubMed]
38. Khawas, P.; Deka, S.C. Isolation and characterization of cellulose nanofibers from bamboo using microwave liquefaction combined with chemical treatment and ultrasonication. *Carbohydr. Polym.* **2016**, *151*, 725–734. [CrossRef]
39. Usmani, Z.; Sharma, M.; Gupta, P.; Karpichev, Y.; Gathergood, N.; Bhat, R.; Gupta, V.K. Ionic liquid based pretreatment of lignocellulosic biomass for enhanced bioconversion. *Bioresour. Technol.* **2020**, *304*, 123003. [CrossRef]
40. Salvaggio, A.; Marino, F.; Albano, M.; Pecoraro, R.; Camiolo, G.; Tibullo, D.; Bramanti, V.; Lombardo, B.M.; Saccone, S.; Mazzei, V.; et al. Toxic effects of zinc chloride on the bone development in Danio Rerio (Hamilton, 1822). *Front. Physiol.* **2016**, *7*, 1–6. [CrossRef]

41. Ciannamea, E.M.; Stefani, P.M.; Ruseckaite, R.A. Physical and mechanical properties of compression molded and solution casting soybean protein concentrate based films. *Food Hydrocoll.* **2014**, *38*, 193–204. [CrossRef]
42. Panthapulakkal, S.; Sain, M. Preparation and characterization of cellulose nanofibril films from wood fibre and their thermoplastic polycarbonate composites. *Int. J. Polym. Sci.* **2012**, *2012*. [CrossRef]
43. Pintiaux, T.; Viet, D.; Vandenbossche, V.; Rigal, L.; Rouilly, A. High pressure compression-molding of α-cellulose and effects of operating conditions. *Materials* **2013**, *6*, 2240–2261. [CrossRef]
44. Cazón, P.; Velazquez, G.; Vázquez, M. Novel composite films from regenerated cellulose-glycerol-polyvinyl alcohol: Mechanical and barrier properties. *Food Hydrocoll.* **2019**, *89*, 481–491. [CrossRef]
45. Bilanovic, D.; Starosvetsky, J.; Armon, R.H. Cross-linking xanthan and other compounds with glycerol. *Food Hydrocoll.* **2015**, *44*, 129–135. [CrossRef]
46. Gogate, P.R.; Shirgaonkar, I.Z.; Sivakumar, M.; Senthilkumar, P.; Vichare, N.P.; Pandit, A.B. Cavitation reactors: Efficiency assessment using a model reaction. *AIChE J.* **2001**, *47*, 2526–2538. [CrossRef]
47. Agarwal, U.P. Raman spectroscopy in the analysis of cellulose nanomaterials. In *Nanocelluloses: Their Preparation, Properties, and Applications*; ACS Publications: Washington, DC, USA, 2017; pp. 75–90. [CrossRef]
48. Biswas, M.C.; Jeelani, S.; Rangari, V. Influence of biobased silica/carbon hybrid nanoparticles on thermal and mechanical properties of biodegradable polymer films. *Compos. Commun.* **2017**, *4*, 43–53. [CrossRef]
49. Johar, N.; Ahmad, I.; Dufresne, A. Extraction, preparation and characterization of cellulose fibres and nanocrystals from rice husk. *Ind. Crops Prod.* **2012**, *37*, 93–99. [CrossRef]
50. Sluiter, A.; Hames, B.; Ruiz, R.; Scarlata, C.; Sluiter, J.; Templeton, D.; Crocker, D. *Determination of Structural Carbohydrates and Lignin in Biomass*; LAP-002 NREL Analytical Procedure; NREL/TP-510-42618; National Renewable Energy Laboratory: Golden, CO, USA, 2004; p. 17.
51. Sun, R.C.; Sun, X.F.; Ma, X.H. Effect of ultrasound on the structural and physiochemical properties of organosolv soluble hemicelluloses from wheat straw. *Ultrason. Sonochem.* **2002**, *9*, 95–101. [CrossRef]
52. Ramadoss, G.; Muthukumar, K. Mechanistic study on ultrasound assisted pretreatment of sugarcane bagasse using metal salt with hydrogen peroxide for bioethanol production. *Ultrason. Sonochem.* **2016**, *28*, 207–217. [CrossRef] [PubMed]
53. Bernal-Lugo, I.; Jacinto-Hernandez, C.; Gimeno, M.; Carmina Montiel, C.; Rivero-Cruz, F.; Velasco, O. Highly efficient single-step pretreatment to remove lignin and hemicellulose from softwood. *BioResources* **2019**, *14*, 3567–3577. [CrossRef]
54. Segal, L.; Creely, J.J.; Martin, A.E.; Conrad, C.M. An empirical method for estimating the degree of crystallinity of native cellulose using the x-ray diffractometer. *Text. Res. J.* **1959**, *29*, 786–794. [CrossRef]
55. Lupoi, J.S.; Gjersing, E.; Davis, M.F. Evaluating lignocellulosic biomass, its derivatives, and downstream Products with Raman spectroscopy. *Front. Bioeng. Biotechnol.* **2015**, *3*, 1–18. [CrossRef]
56. Agarwal, U.P.; Reiner, R.R.; Ralph, S.A. Estimation of cellulose crystallinity of lignocelluloses using near-IR FT-Raman spectroscopy and comparison of the Raman and segal-WAXS methods. *J. Agric. Food Chem.* **2013**, *61*, 103–113. [CrossRef]
57. Lupoi, J.S.; Singh, S.; Simmons, B.A.; Henry, R.J. Assessment of lignocellulosic biomass using analytical spectroscopy: An evolution to high-throughput techniques. *Bioenergy Res.* **2014**, *7*, 1–23. [CrossRef]
58. Sacui, I.A.; Nieuwendaal, R.C.; Burnett, D.J.; Stranick, S.J.; Jorfi, M.; Weder, C.; Foster, E.J.; Olsson, R.T.; Gilman, J.W. Comparison of the properties of cellulose nanocrystals and cellulose nanofibrils isolated from bacteria, tunicate, and wood processed using acid, enzymatic, mechanical, and oxidative methods. *ACS Appl. Mater. Interfaces* **2014**, *6*, 6127–6138. [CrossRef] [PubMed]
59. Alves, A.P.P.; de Oliveira, L.P.Z.; Castro, A.A.N.; Neumann, R.; de Oliveira, L.F.C.; Edwards, H.G.M.; Sant'Ana, A.C. The structure of different cellulosic fibres characterized by Raman spectroscopy. *Vib. Spectrosc.* **2016**, *86*, 324–330. [CrossRef]
60. Ma, P.; Lan, J.; Feng, Y.; Liu, R.; Qu, J.; He, H. Effects of continuous steam explosion on the microstructure and properties of eucalyptus fibers. *BioResources* **2016**, *11*, 1417–1431. [CrossRef]
61. Rezende, C.A.; De Lima, M.; Maziero, P.; Deazevedo, E.; Garcia, W.; Polikarpov, I. Chemical and morphological characterization of sugarcane bagasse submitted to a delignification process for enhanced enzymatic digestibility. *Biotechnol. Biofuels* **2011**, *4*. [CrossRef] [PubMed]
62. Yang, H.; Yan, R.; Chen, H.; Lee, D.H.; Zheng, C. Characteristics of hemicellulose, cellulose and lignin pyrolysis. *Fuel* **2007**, *86*, 1781–1788. [CrossRef]

63. Yildirim, N.; Shaler, S. A study on thermal and nanomechanical performance of Cellulose Nanomaterials (CNs). *Materials* **2017**, *10*, 718. [CrossRef]
64. Meng, Q.; Wang, T.J. Mechanics of strong and tough cellulose nanopaper. *Appl. Mech. Rev.* **2019**, *71*. [CrossRef]
65. Ghaderi, M.; Mousavi, M.; Yousefi, H.; Labbafi, M. All-cellulose nanocomposite film made from bagasse cellulose nanofibers for food packaging application. *Carbohydr. Polym.* **2014**, *104*, 59–65. [CrossRef]
66. Mosier, N.; Wyman, C.; Dale, B.; Elander, R.; Lee, Y.Y.; Holtzapple, M.; Ladisch, M. Features of promising technologies for pretreatment of lignocellulosic biomass. *Bioresour. Technol.* **2005**, *96*, 673–686. [CrossRef]
67. Sun, S.; Mitchell, J.R.; MacNaughtan, W.; Foster, T.J.; Harabagiu, V.; Yihu Song, A.; Zheng, Q. Comparison of the mechanical properties of cellulose and starch films. *Biomacromolecules* **2010**, *11*, 126–132. [CrossRef] [PubMed]
68. Park, S.; Baker, J.O.; Himmel, M.E.; Parilla, P.A.; Johnson, D.K. Cellulose crystallinity index: Measurement techniques and their impact on interpreting cellulase performance. *Biotechnol. Biofuels* **2010**, *3*, 10. [CrossRef] [PubMed]
69. Abdel-Halim, E.S. Chemical modification of cellulose extracted from sugarcane bagasse: Preparation of hydroxyethyl cellulose. *Arab. J. Chem.* **2014**, *7*, 362–371. [CrossRef]
70. Gierlinger, N.; Keplinger, T.; Harrington, M.; Schwanninger, M. Raman imaging of lignocellulosic feedstock. *Cellul. Biomass Convers.* **2013**. [CrossRef]